

Article

Production and Characterisation of Pickering Emulsions Stabilised by Colloidal Lignin Particles Produced from Various Bulk Lignins

Julia Tomasich ^{1,2,*} , Stefan Beisl ²  and Michael Harasek ¹ ¹ Institute of Chemical, Environmental and Bioscience Engineering, TU Wien, 1060 Vienna, Austria² Lignovations GmbH, 3400 Klosterneuburg, Austria

* Correspondence: julia.tomasich@tuwien.ac.at

Abstract: The use of lignin, an abundant phenolic bio-polymer, allows us to transform our fossil-based economy into a sustainable and bio-based economy. The transformation of bulk lignin into colloidal lignin particles (CLPs) with well-defined surface chemistry and morphology is a possible way to cope with the heterogeneity of lignin and use it for material applications. These CLPs can be used as emulsifiers in so-called Pickering emulsions, where solid particles stabilise the emulsion instead of environmentally harmful synthetic surfactants. This work investigates the application of CLPs produced from various bulk lignins as a stabiliser in o/w Pickering emulsions with two different oil phases (solid and liquid state). The CLPs had a primary particle size of 28 to 55 nm. They were successful in stabilising oil-in-water Pickering emulsions with high resistance to coalescence and a strong gel-like network. This enables novel applications for CLPs in the chemical and cosmetic industries, and can replace fossil-based and synthetic ingredients.

Keywords: lignin; colloidal particles; Pickering emulsion; rheological behaviour



Citation: Tomasich, J.; Beisl, S.; Harasek, M. Production and Characterisation of Pickering Emulsions Stabilised by Colloidal Lignin Particles Produced from Various Bulk Lignins. *Sustainability* **2023**, *15*, 3693. <https://doi.org/10.3390/su15043693>

Academic Editors: Oz Sahin and Russell Richards

Received: 3 January 2023

Revised: 10 February 2023

Accepted: 14 February 2023

Published: 16 February 2023



Copyright: © 2023 by the authors. Licensee MDPI, Basel, Switzerland. This article is an open access article distributed under the terms and conditions of the Creative Commons Attribution (CC BY) license (<https://creativecommons.org/licenses/by/4.0/>).

1. Introduction

Driven by concerns about climate change, environmental pollution, and the exhaustion of fossil fuels, interest in biobased products has risen dramatically in the past years. Since biobased products cost more than those produced from non-renewable resources [1], lignocellulosic biorefineries are designed to meet the challenges of combining renewable feedstock and industrial production technologies [2]. The raw materials for these biorefinery concepts are straw, wood or grass consisting of cellulose, hemicellulose, and lignin [2]. Currently, polysaccharides are utilised to produce biofuel or other chemical products [3], whereas lignin is underutilised, and around 40% of the lignin is traditionally burned to generate energy for the biorefinery process [3,4].

Lignin accounts for around 15–30 wt% of the total dry matter of woody and non-woody plants and, thus, is the second-most abundant renewable biopolymer [4]. Depending on the plant source, the complex molecular structure is given by the different amounts of its primary monolignols, p-coumaryl alcohol, coniferyl alcohol, and sinapyl alcohol, which result in p-hydroxyphenyl (H), guaiacyl (G), and syringyl (S) lignin subunits linked by both carbon–carbon and ether bonds [3,4]. According to the presence of the three monolignols in lignin from different plants, it is roughly classified into softwood lignin (mainly coniferyl alcohol), hardwood lignin (coniferyl and sinapyl alcohol), and grass lignin (all three alcohols) [5]. Furthermore, the extraction or pre-treatment processes lead to additional structural changes and modifications of functional groups, making lignin valorisation even more challenging [3,6,7]. Lignin produced by commercial pulp and paper processes, such as kraft lignin or lignosulfonates, contains high amounts of sulphur. In contrast, organosolv lignin, steam explosion lignin, soda/alkali lignin, and enzymatic hydrolysis lignin (EH) are isolated without sulphur in pilot-scale processes [6,8].

Despite this challenging heterogeneity caused by its natural and technical origin, the outstanding physicochemical properties of lignin make it worthwhile to investigate methods to valorise the obtained technical lignins. These properties include biodegradability; UV absorbance; good mechanical properties, such as high stiffness; antioxidation characteristics; and resistance to microbial and fungal attacks. Furthermore, lignin contains both hydrophobic and hydrophilic groups [4,6,8,9].

Due to the physicochemical properties and the availability of lignin, the technical, economic, environmental, and socio-economic dependencies have been investigated in the literature. Chauhan et al. [10] reviewed the application of lignin in various sectors and showed that the usage of this aromatic biopolymer is essential for bioeconomy and sustainability. In order to achieve further value addition to this feedstock, an investigation of lignins' usage and valorisation has to be conducted.

One possible way to valorise technical lignins and to cope with the heterogeneity of lignin is the transformation into colloidal lignin particles (CLPs) with well-defined surface chemistry and morphology [11–13]. In literature, several production methods for CLPs are described [4,8,12,14,15]. The CLPs utilised in this work were produced by the method of solvent shifting, during which the lignin solubility was decreased by the continuous addition of the anti-solvent (water) [11,16]. The thus-formed particles are received in aqueous, highly concentrated dispersions, ready for numerous applications. Österberg et al. [12] and Beisl et al. [17] summarised the various fields of application for these spherical particles produced by the solvent shift method.

One of the described applications is the utilisation of CLPs as an emulsifier in so-called Pickering emulsions. These so-called Pickering emulsions can be any type of emulsion stabilised by solid particles instead of surfactants [18]. Due to their stability against coalescence and better biocompatibility, Pickering emulsions can be applied in a broad range of fields [19]. Yu et al. [20] and Saberi Riseh et al. [21] showed that encapsulation of pesticides and biocontrol of bacteria are of interest. Taking advantage of the properties of Pickering emulsions, green materials can be used to stabilise agrochemicals or drugs and, furthermore, control their release [20,22]. Another field where Pickering emulsions stabilised by lignin particles are relevant is the cosmetic industry. The properties of lignin mentioned above make it worthwhile to use the CLPs as a natural ingredient in sunscreens to protect human skin from UV irradiation [23,24]. The present study demonstrates the possibility of valorising different technical or bulk lignins produced from various feedstocks. The heterogeneity of the different bulk lignins is decreased by transforming them into CLPs with similar properties. This valorisation step enables lignin, to be used instead of synthetic surfactants, to stabilise droplets in emulsions.

This work investigates the properties of CLPs from different bulk lignins and their ability to stabilise oil-in-water (o/w) Pickering emulsions. Five bulk lignins (organosolv, alkali, and three enzymatically hydrolysed) were dissolved, precipitated into CLPs, and concentrated. The resulting particles were analysed for their particle size, molecular weight, and water contact angle. The Pickering emulsion was prepared by mixing the CLP suspensions with two different oil phases under a high shear rate. The produced emulsions were investigated in terms of rheological behaviour and stability. Furthermore, the emulsions were analysed by fluorescence microscopy to identify the CLPs as emulsifiers in the formed emulsions.

2. Materials and Methods

In this work, CLP suspensions were produced from different bulk lignins, cleaned, and concentrated. The suspensions were analysed by scanning electron microscopy (SEM), dynamic light scattering (DLS), high-performance size exclusion chromatography (HPSEC), and contact angle measurement. Pickering emulsions were produced with two types of oils and aqueous CLP suspensions. Stability tests, rheological investigation, and fluorescence microscopy were performed to analyse the different lignins in terms of their performance as an emulsifier.

2.1. Materials

To produce the CLP suspensions, the following materials were used: organosolv lignin (OS) (beech wood, Fraunhofer CBP, Leuna, Germany), alkali lignin (AL) (grass, Protobind 1000, PIT Innovations, Rüschtikon, Switzerland), three different enzymatic hydrolysis lignins originating from birch (EH1) and beech wood (EH2 and EH3), ethanol (EtOH) (96 wt%, AustrAlco GmbH, Spillern, Austria), and ultra-pure water (18 M Ω /cm). The emulsions were prepared with shea butter (refined and deodorised), babassu oil (cold-pressed and refined) (oil phase 1), and MCT oil (oil phase 2) purchased at Naturkosmetik Werkstatt OG, Linz, Austria.

2.2. Preparation of CLP Suspensions

The bulk lignins were dissolved in aqueous ethanol (60 wt%) and filtered. Out of these solutions, CLPs were formed by decreasing the solubility of lignin in the medium with the addition of water in a static mixer, as described by Beisl et al. [11]. In order to increase the concentration of the precipitated particles, lower the remaining ethanol concentration, and remove the dissolved lignin and impurities in the suspension, ultrafiltration in diafiltration mode was performed according to the method described in a previous work by Miltner et al. [25]. To eliminate the influence of the lignin particle concentration on the emulsification property, the particle concentration was set to a concentration of 4.85 wt% for all suspensions. The production of the CLP suspensions was conducted in cooperation with Lignovations GmbH, Tulln/Donau, Austria.

2.3. CLP Characterisation

2.3.1. Particle Size and Morphology

The hydrodynamic diameter and size distribution in the aqueous suspension were determined with a Litesizer 500 (Anton Paar GmbH, Graz, Austria) using dynamic light scattering (DLS). The refractive index of the CLPs was set to 1.53 and the imaginary refractive index to 0.1; the given values are averages and standard errors of three separate measurements.

The primary particle size and the morphology of the CLPs were analysed with a scanning electron microscope (SEM) (Quanta 200 FEG-SEM, Fei, Hillsboro, OR, USA) at an acceleration voltage of 5 kV. The samples were sputtered 2 times with 4 nm Au/Pd (60:40 wt%) before measurement. The primary particle size was manually evaluated with ImageJ software, and the given values are averages and standard errors from 150 counts.

2.3.2. Contact Angle Measurement

Microscope glass slides were treated with piranha solution (H₂SO₄ 96%:H₂O₂ (30%) 3:1) for 30 min, then cleaned with ultra-pure water followed by EtOH (100%, Chem-Lab NV, Zedelgem, Belgium), and then left to dry. These slides were dip-coated with CLP suspension three times to achieve a uniform coating. The wettability of colloidal CLPs was determined by sessile-drop contact angle measurement using distilled water in a tensiometer (Attension Theta Flex Auto 4, Gothenburg, Sweden). The dosing volume of each drop was 5 μ L, controlled by both a precise dispenser and drop image analysis.

2.3.3. Molecular Weight

The molecular mass distribution of the CLPs was investigated with an alkaline high-performance size exclusion chromatography (HPSEC) using 10 mM NaOH as an eluent. Three columns, in series, at 40 °C (PW5000, PW4000, PW3000; TOSOH Bioscience, Darmstadt, Germany) were used with an Agilent 1200 HPLC system (flow rate: 1 mL/min, DAD detection at 280 nm, Santa Clara, CA, USA). The particle suspensions were diluted with ultra-pure water, and the pH was adjusted by NaOH to reach the same concentration as the eluent. The calibration of the columns was performed using polystyrene sulfonate reference standards (PSS GmbH, Mainz, Germany) with molar masses at 78,400 Da, 33,500 Da, 15,800 Da, 6430 Da, 1670 Da, 891 Da, and 208 Da at peak maximum.

2.4. Preparation of o/w Pickering Emulsions

Pickering emulsions were produced by mixing two different oil phases with the aqueous phase containing the CLPs (4.85 wt%) as an emulsifier, using the same weight ratio (1:1), for a total amount of 100 g. The first oil phase (1), containing shea butter and babassu oil (weight ratio 1:1), was heated up to ~50 °C and melted, whereas the MCT oil was simply weighed at room temperature. Emulsification was performed with an Ultra Turrax T25 equipped with the dispersing tool S 25 KD—25 G (IKA-Werke GmbH&Co.KG, Staufen, Germany) by continuously adding the oil phase into the CLP suspension during mixing at 12,000 rpm for 2 min. The emulsions containing shea/babassu were mixed at 37 °C due to the given melting point of the oil phase, whereas the emulsions containing MCT oil were mixed at room temperature. Parts of the prepared Pickering emulsions were poured into glass centrifuge tubes and left covered and without sunlight for 24 h to stabilise. The remaining emulsions were stored in closed plastic bottles.

2.5. Pickering Emulsion Characterisation

2.5.1. Stability Test

The Pickering emulsions were centrifuged to investigate their stability to coalescence using a benchtop centrifuge equipped with a swinging bucket rotor (Sigma centrifuge 4–16KS, rotor 11660; Sigma Laborzentrifugen GmbH, Osterode am Harz, Germany) at a relative centrifugal force (RCF) of 500 g for 10 min, and directly thereafter, at RCF 1000 g for 10 min. The volume of the separated phase was measured to determine and compare the relative stability of the emulsions.

2.5.2. Fluorescence Microscopy

The Pickering emulsions were imaged using a polarisation microscope (Nikon Upright Eclipse Ci, objective Plan Apo λ 40x/0.95 equipped with a Nikon LV-UEPI2 Universal Epi Illuminator 2, Long Island, NY, USA) using a FITC filter with a range from 465–495 nm for excitation and 515–555 nm for emission. The emulsion was placed on a microscope glass covered by a coverslip with a spacer in between. The droplet size of the emulsions was manually evaluated with ImageJ software, where at least 100 droplets were measured for each droplet size distribution.

2.5.3. Rheological Tests

All rheological analyses were performed using a plate–plate rheometer (MCR300 SN621304, measuring system PP25, Anton Paar GmbH, Germany, gap size 1 mm, Rheo-plus/32 Multi3 V3.40). The temperature was set to 25 °C by a Peltier lower plate. The emulsion's linear viscoelastic region (LVE) was determined with an amplitude sweep test using a constant angular frequency (strain $\gamma = 0.01$ –10%, angular frequency $\omega = 10$ 1/s). As a function of the LVR, a frequency sweep test was performed to investigate the trend of the storage and loss modulus of the emulsions with constant deformation (amplitude strain = 1%). Additionally, a dynamic viscosity measurement was carried out within a specific shear rate region (0.0001–0.02 1/s).

3. Results and Discussion

3.1. CLP Suspensions

Solutions of five different bulk lignins in aqueous ethanol (60 wt%) were prepared, from which CLP suspensions were obtained by the addition of an anti-solvent in a static mixer. The suspensions were purified and concentrated in membrane filtration steps. The produced CLPs were chemically and physically characterised by dynamic light scattering, SEM imaging, HPLC, and contact angle measurements with water.

The hydrodynamic diameter (HD) resulting from DLS measurements showed significant differences for the CLPs produced by the different bulk lignins (Figure 1). The result of EH1 CLPs showed a minimum HD of 80 nm (± 0.5 nm), followed by EH2 and EH3 CLPs

with 108 nm (± 4 nm) and 110 nm (± 0.4 nm), whereas particles produced from OS lignin and AL showed distinctly higher HD values, around 300 nm.

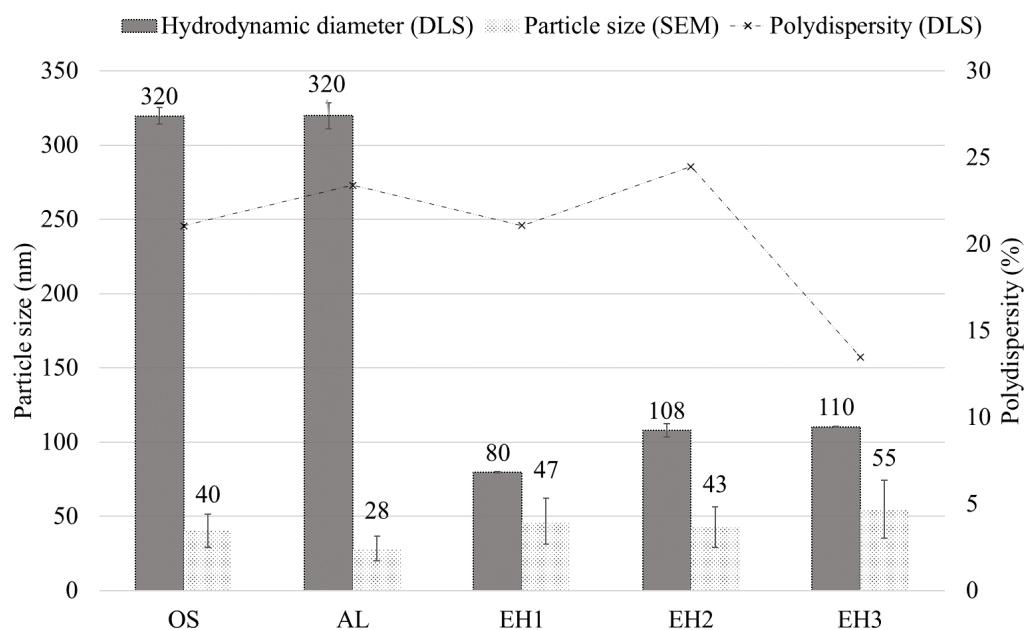


Figure 1. Hydrodynamic diameter and polydispersity (DLS) of CLPs and primary particle size average (SEM).

To compare them with these results, the primary particles were also analysed. A primary particle was assumed to be identifiable as a constituent particle in aggregates or agglomerates with a spherical shape. The size of the primary particles, evaluated by manual measurement of the CLPs from the SEM images (Figure 2), showed a significant difference from the HD results. However, the order of magnitude of the primary particle size was similar for the different CLPs, ranging from 28 nm (± 8 nm) for AL to 55 nm (± 20 nm) for EH3. The difference between the hydrodynamic diameters obtained by DLS measurement and the primary particle size obtained by evaluation of the SEM images could be explained by agglomeration or aggregation of the primary particles. CLPs produced from AL comprising the smallest primary particles result in agglomerates with HDs of 320 nm (± 9 nm), while CLPs with primary particle sizes of 55 nm (EH3) form smaller agglomerates with HDs of 110 nm. This result coincides with the theory of Zhang et al. [26] that agglomeration occurs due to the greater surface energy of smaller particles and, consequently, a stronger hydrogen bonding effect. However, data in Figure 1 further show a dependency of agglomeration formation on the bulk lignin's origin, since particles produced from EH lignin show a lower tendency to agglomerate than CLPs from OS and AL.

In Figure 3, the mass-averaged molecular weights (M_w) and polydispersity indices (PDIs) of the CLPs are presented. Comparing the trend of the CLPs' molecular weight, only small differences are noticeable. M_w s for the CLPs all result between 1691 Da (EH3) to 1914 Da (OS). The varying M_w s for the three CLPs produced by EH might be explained by different conditions during the enzymatic hydrolysis processes.

Colloidal lignin particles tend to stabilise oil-in-water (o/w) or water-in-oil Pickering emulsions, depending on their hydrophilicity or hydrophobicity [27,28]. CLPs with contact angles $\theta_{H_2O} < 90^\circ$ are preferentially wetted by the aqueous phase and build an adsorbent layer around the oil droplets due to their hydrophilicity [29]. The results shown in Table 1 indicate that the produced CLPs are hydrophilic, with contact angles ranging from 31.4 to 45.1°. The contact angle for AL CLPs, compared to OS CLPs, exhibits slightly higher values, suggesting that this led to the generation of smaller primary particles for AL due to the hydrophilicity [26]. The three CLPs produced from EH show strongly varying

contact angles, from 31.4°(EH3) to 38.1(EH1) to 45.1°(EH2). This leads back to the results of molecular weight distribution, where the highest M_w from EH CLPs was indicated for EH2 and the lowest M_w for EH1 (Figure 3), suggesting that the M_w distribution influences the contact angle slightly, comparing the enzymatically hydrolysed lignins.

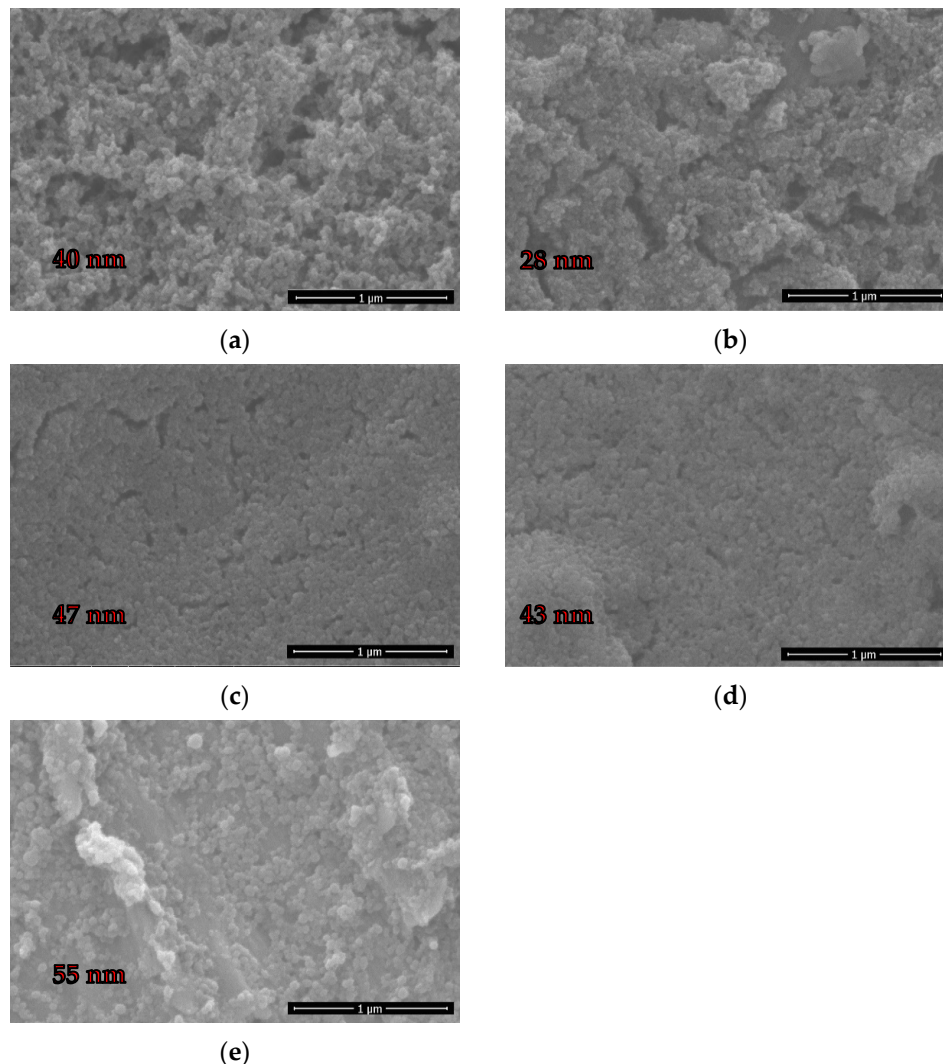


Figure 2. SEM images of OS (a), AL (b), EH1 (c), EH2 (d), and EH3 (e) CLPs.

Table 1. Contact angle of water on CLPs.

	Contact Angle (°)
OS	37.1 ± 3.3
AL	34 ± 3.1
EH1	38.1 ± 3.1
EH2	45.1 ± 3.3
EH3	31.4 ± 1.5

3.2. Pickering Emulsions

The Pickering emulsions were prepared by mixing CLP suspensions with an oil phase (mass ratio 1:1) and applying high shear rates. The two oil phases were a 1:1 mixture of shea butter and babassu oil (solid state) and MCT oil (liquid state), respectively, at room temperature. The mixture of babassu oil and shea butter was chosen to represent the oil/fat phase of cosmetic creams. To investigate the ability of the produced CLPs to stabilise o/w emulsions, centrifugation at different RCFs (500 g, 1000 g) was conducted.

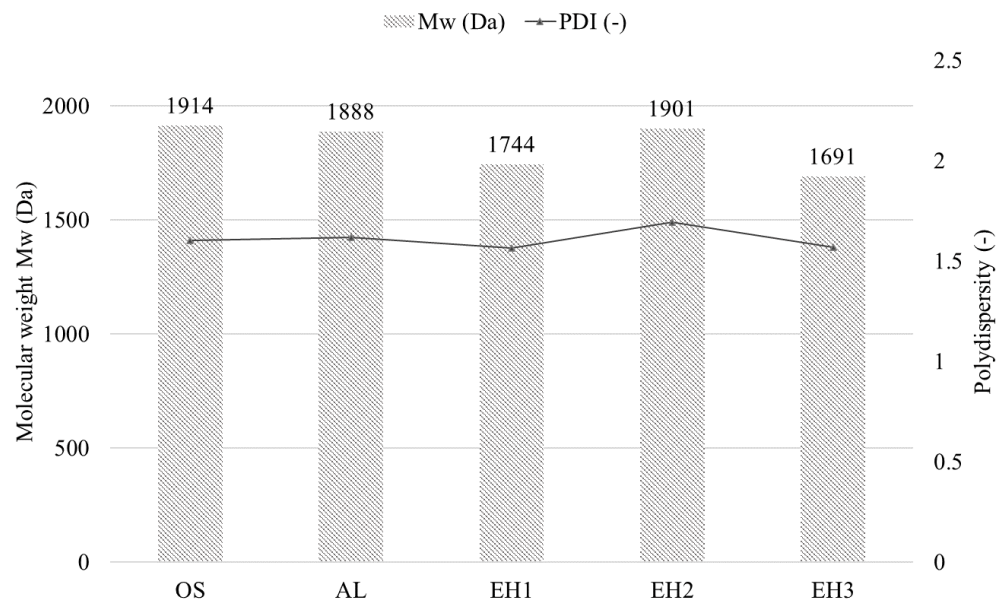


Figure 3. M_w with the PDI of the different CLP suspensions.

The molecular structure of lignin, with its mainly hydrophilic and minor hydrophobic parts, result in water contact angles of 35–45°, as mentioned in 3.1. This property is accountable for stabilising the o/w Pickering emulsions because the water phase wets the CLPs, and the minor hydrophobic part of the particle makes it possible to attach to the oils phase, therefore stabilising the oil drop in the continuous water phase [19,28]. The particle size and morphology of primary particles also influence the ability to stabilise emulsions [19].

Directly after the emulsification, all samples were homogeneous and showed no segregation. For stability monitoring, a 7 mL sample of each emulsion was put into a centrifugation tube. First, segregation of the water phase, below the homogeneous emulsion layer, was observed after 24 h for the three emulsions prepared with EH and MCT oil. The segregation volume was monitored after each centrifugation procedure and is shown in Figure 4. Interestingly, only segregation of the water phase was observed, and the emulsion was resting on top of the segregated aqueous phase (Figure 5). This could be an indication of a stable dispersion of the oil droplets by the CLPs and good resistance to coalescence.

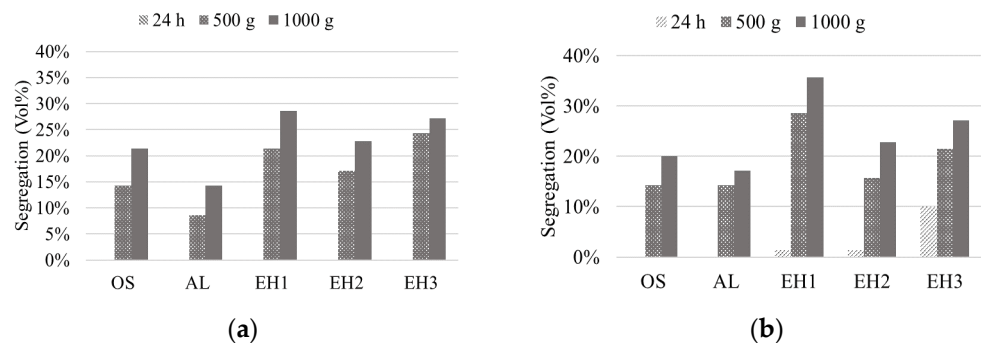


Figure 4. Segregation of the water phase of prepared Pickering emulsions with different CLP suspensions and shea/babassu oil (a) and MCT oil (b), before and after centrifugation at 500 g and 1000 g.

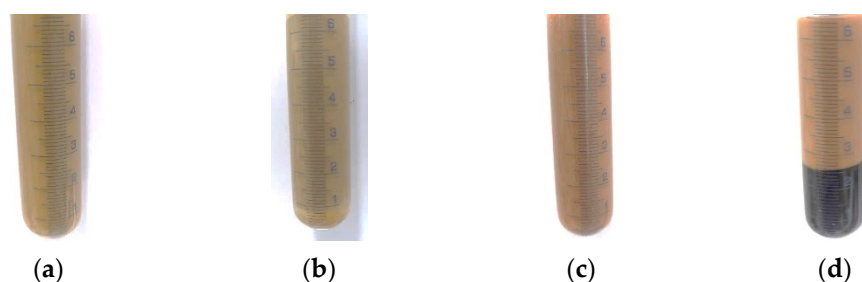


Figure 5. Emulsions with shea/babassu and AL after 24 h (a) and after centrifugation at 1000 g (b); emulsions prepared with MCT and EH1 after 24 h (c) and centrifugation at 1000 g (d).

Despite the strong particle agglomeration in the suspensions of OS and AL, those two CLP suspensions formed the most stable emulsions according to the stability test result. The highest coalescence and segregation were observed for the emulsions stabilised by CLP suspension EH1. Comparing the two different oil phases, the emulsions prepared with MCT oil already showed a higher tendency for segregation before the centrifugation step. Nevertheless, the remaining emulsion phases showed comparable segregation behaviour to the emulsions prepared with shea/babassu oil. In Figure 5, AL CLP-stabilised emulsions and EH1 CLP-stabilised emulsions are shown before and after centrifugation. Overall, the results of the stability tests suggest that all emulsions contain a phase with a strong network of dispersed droplets, demonstrating stability at 1000 g.

Moreover, the droplet size of the o/w emulsions was evaluated by measuring the drops shown in images taken by fluorescence microscopy (Figure 6). Due to the fluorescence of lignin molecules [30], the taken fluorescence microscopy images show oil droplets surrounded by CLPs. The average droplet size can be found in Table 2. However, no general correlation between droplet size and emulsion stability was identified.

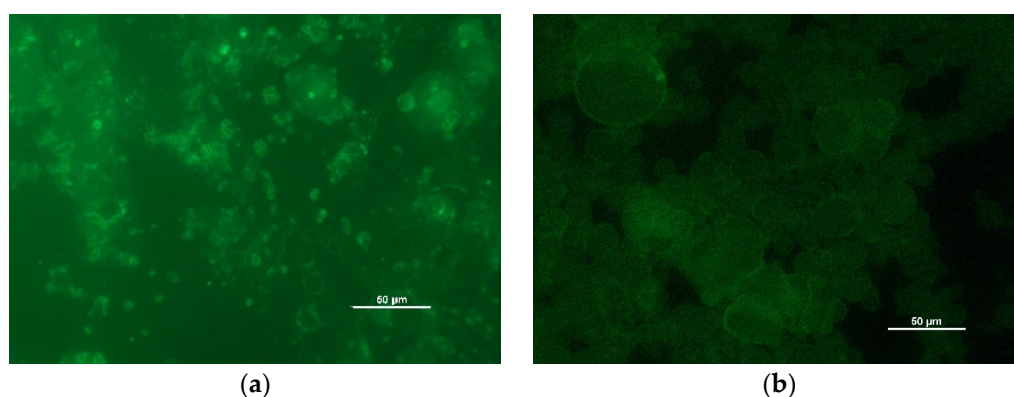


Figure 6. Images taken by fluorescence microscopy: OS shea/babassu (a), EH1 MCT (b).

Table 2. Droplet size of the emulsions measured from fluorescence images.

	Droplet Size (μm)				
	OS	AL	EH1	EH2	EH3
Shea/Babassu	6.72 ± 2.83	9.06 ± 2.56	3.81 ± 2.22	5.01 ± 2.41	5.11 ± 2.51
MCT	5.01 ± 3.38	2.96 ± 0.84	6.20 ± 2.99	5.59 ± 2.11	4.43 ± 2.78

The rheological behaviour of emulsions provides information about their structure, the properties of the components, and their stability [31]. Therefore, the prepared emulsions were investigated concerning their viscosity over a specific shear rate and analysed by oscillatory tests.

The amplitude sweep test was performed to find the linear viscoelastic (LVE) region of the emulsions, where the structure of the sample is intact. The tests were performed

by applying oscillatory strain over a continuous rising amplitude (0.01–10%) at a fixed frequency (10 1/s) while recording the values of the storage (G') and loss (G'') modulus. The maximum amplitude allowed for the emulsions can be derived by plotting the complex modulus G^* , calculated from the storage and loss modulus (Equation (1)), over the deformation amplitude (γ).

$$|G^*| = \sqrt{(G')^2 + (G'')^2} \quad (1)$$

The maximum value for the deformation amplitude γ was ascertained from the data plotted in Figure 7 in order to stay dependent on the linear viscoelastic region, according to the evaluation process explained in the literature [31,32]. The point of the critical deformation amplitude is marked in both plots (Figure 7) at $\gamma_{crit.} = 1.2\%$.

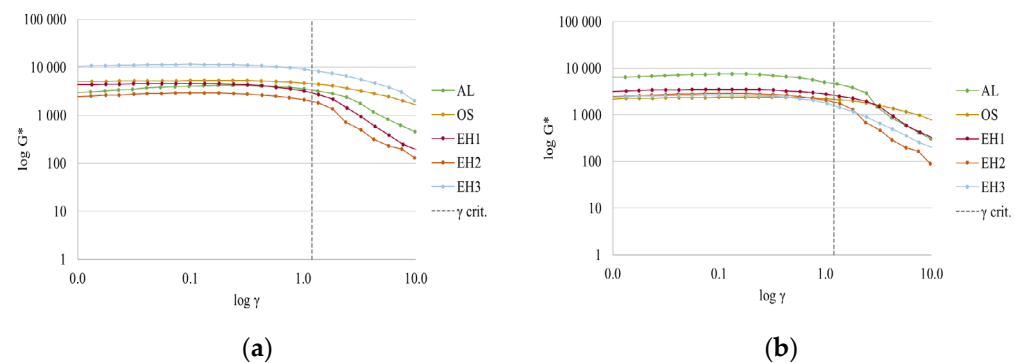


Figure 7. Amplitude sweep test of CLP emulsions with shea/babassu (a) and MCT oil (b) to determine the LVE region.

The frequency sweep tests are dynamic oscillatory measurements that give information about the viscous and elastic behaviour of a viscoelastic system. Referring to the result from the amplitude sweep test, frequency sweep tests were carried out at the deformation amplitude γ of 1% to obtain the storage (G') and loss (G'') modulus of the emulsions. The moduli indicate a strong or weak network formation of dispersed droplets in emulsions and, therewith, elastic or viscous behaviour. A strong network is indicated by the fulfilment of the criteria $G' > G''$ and both moduli being independent of frequency. The ratio of the moduli is shown in Figure 8a,b by plotting the loss factor $\tan\delta$ (Equation (2)) [33]. A low and constant loss factor implies an elastic response of the emulsions under shear stress and, therefore, a higher developed gel-like colloidal network [34].

$$\tan\delta = \frac{G''}{G'} \quad (2)$$

The emulsions prepared with shea/babassu showed a similar behaviour during the frequency sweep, and the loss factor remained relatively constant, except for that of the emulsion prepared by CLP suspension EH1 (Figure 8a). The low and frequency-independent values of the loss factor for the OS, AL, EH2, and EH3 formulations indicate an elastic response of the emulsion and, thus, the appearance of a gel-like colloidal network. In Figure 8c, the two moduli are plotted for the emulsion prepared by AL (green) and EH1 (purple) with shea/babassu. The AL emulsion shows an almost independent trend of the moduli and the fulfilment of the criteria for stable emulsions $G' > G''$ over the applied angular frequency. Hence, an elastic response to the applied shear stress is given due to the existence of a strong network of dispersed droplets stabilised by particles. This result coincides with the stability tests of the emulsions (Figure 4a), where the segregation volume for AL emulsion was very low. The findings for the frequency sweep tests performed using the emulsions prepared with CLP suspensions OS, EH2, and EH3 (Figure 8e) showed similar behaviour. On the other hand, the trend of the moduli (Figure 8c), as well as the trend of the loss factor (Figure 8a) for the shea/babassu emulsion prepared with CLP suspension

EH1, strongly depend on the frequency, and the values of the moduli are related to each other ($G' \sim G''$). In addition, this result agrees with the stability tests mentioned above.

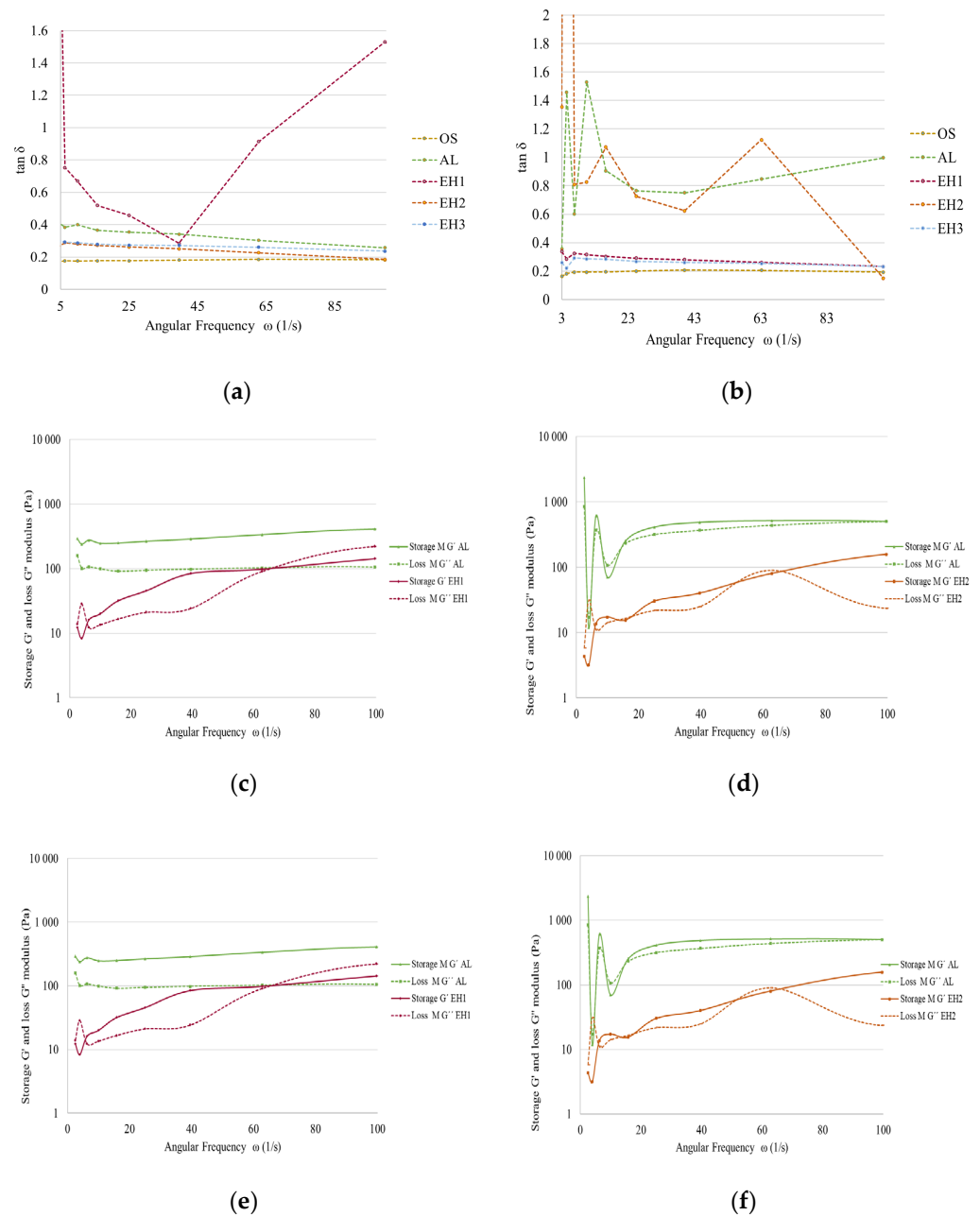


Figure 8. Loss factor resulting from frequency sweep tests with shea/babassu emulsions (a) and MCT emulsions (b); storage and loss modulus of shea/babassu with AL and EH1 (c); storage and loss modulus MCT with AL and EH2 (d); storage and loss modulus of shea/babassu with EH2, EH3, and OS (e); storage and loss modulus of MCT with EH1, EH3, and OS (f).

The loss factor results for the emulsions prepared with MCT oil show frequency independence and low values for the CLP suspensions EH1, EH3, and OS (Figure 8b). The loss factor of the emulsions prepared with AL showed strong dependence at low frequencies and lower dependence at higher frequencies. The loss factor of the emulsion prepared with CLP suspension EH2 strongly depended on the frequency (Figure 8b). In Figure 8d, the dependence of the moduli on the frequency for EH2 is highlighted even more, as is the failure to perform the criteria $G' > G''$ for this emulsion. The trend of the moduli for the AL emulsion also shows dependence on the frequency, but fulfils the criterion of G'

$> G''$ over a certain frequency. The frequency sweep test for the emulsions prepared with MCT oil and CLP suspensions OS, EH1, and EH3 results in frequency-independent moduli, and the data fulfil the criteria $G' > G''$, indicating strong networks and elastic response to shear stress. These rheological data do not agree entirely with the results of the stability tests carried out in the centrifuge (Figure 4b), which might be due to the different physical properties of MCT oil compared to the other oil phase, which consisted of shea butter and babassu oil.

Furthermore, the emulsions stabilised by OS CLP suspensions demonstrated the best long-term stability with shea/babassu as well as with MCT oil. This circumstance coincides well with the very low loss factor, which also shows almost no dependence on the frequency for both emulsions (Figure 8a,b), as well as frequency-independent moduli fulfilling the criteria $G' > G''$.

Emulsions commonly exhibit non-Newtonian properties, where the viscosity is a function of the shear rate. Furthermore, these non-Newtonian fluids show shear-thinning behaviour, by which the viscosity decreases as the shear rate increases [35].

The viscosity measurements were performed at very low shear rates (0.0002–0.02 1/s). In Figure 9, the viscosity trends of the shea/babassu emulsions (a) and the MCT emulsions (b) are shown. The non-Newtonian and shear-thinning behaviour can be observed for all emulsions. Furthermore, according to Derkach [36], the viscosity is strongly dependent on the particle size of the stabilising particles in Pickering emulsions. High viscosity values are achieved by small stabilising particles. The results indicate that some of the agglomerates measured by DLS (OS and AL CLPs Figure 1) might disperse during the emulsion formation due to the high viscosity of the emulsions with shea/babassu and MCT, which were stabilised by OS CLP suspension. The high viscosity is another explanation of the observed long-term stability of the OS emulsions.

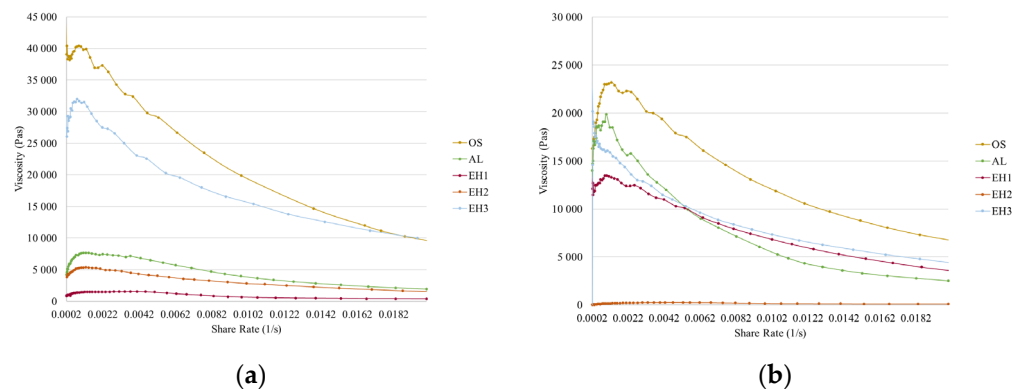


Figure 9. Viscosity of the emulsions prepared with shea/babassu (a) and MCT (b).

The comparison of the results from the frequency sweep and viscosity measurements shows a consensus. Looking at the emulsion with shea/babassu stabilised by CLP suspension EH1, the low viscosity (Figure 9a) coincides with the results from the frequency sweep test (Figure 8a,c). In addition, the results for the emulsion with MCT stabilised by EH2 show accordance. Furthermore, the viscosity values, as well as the results from the frequency sweep test concerning the emulsions stabilised by EH3, OS, and AL, indicate a strong network of disperse drops stabilised by small particles.

4. Conclusions

The production and characterisation of colloidal lignin particles from different bulk lignins, followed by the preparation of o/w Pickering emulsions stabilised by those CLPs, were performed in the present work. The transformation of the bulk lignins into CLPs resulted in particles with similar primary particle sizes (27–54 nm) and molecular weights in the same range (1691 Da–1914 Da) with relatively low PDIs. The measurement of the

contact angle with water allowed the first indication of the ability of the CLPs to stabilise o/w Pickering emulsions. All CLPs showed hydrophilic properties, with contact angles from 31.4 to 45.1°. The agglomeration of OS and AL CLPs does not affect their ability to stabilise o/w Pickering emulsions.

Pickering emulsions containing a shea butter/babassu oil mixture, as well as MCT oil, were characterised through stability tests, fluorescence microscopy, and rheological analyses. Emulsions containing shea/babassu showed slightly higher stability than those stabilised by MCT oil, suggesting that this is an effect of their different aggregate phases at room temperature. Moreover, according to the stability tests, the CLPs produced by OS and AL lignin exhibited a better performance as emulsifiers than the EH CLPs. Moreover, only the segregation of water was observed, indicating a stable droplet network and a high resistance to the coalescence of the oil phase.

The linear viscoelastic region was ascertained by performing an amplitude sweep test for all prepared emulsions. The critical deformation amplitude was found to be 1.2%. Hence, the oscillatory frequency sweep tests were performed at an amplitude of 1%. Physical stability and a gel-like colloidal network of the emulsions with shea/babassu stabilised by AL, OS, EH2, and EH3, and with MCT oil stabilised by OS, EH1, and EH3, were observed. Non-Newtonian and shear-thinning behaviour, of all emulsions were proven in the viscosity measurements.

Overall, the use of several different bulk lignins to produce CLPs, as well as the subsequent preparation of o/w emulsions, was successful. The transformation of bulk lignins into colloidal particles made it possible to obtain particles with similar properties. The valorisation of various bulk lignins from different feedstocks by producing CLPs revealed the opportunity to overcome the heterogeneity of available lignins. This is an essential step concerning the need to replace synthetic or fossil fuel-based materials to make a step towards a biobased economy. The ability of the produced CLPs to stabilise the prepared o/w Pickering emulsions showed their potential to serve as emulsifiers in different application fields. The replacement of synthetical surfactants in the cosmetic industry would be an improvement concerning human health and environmental friendliness.

Author Contributions: Conceptualization, J.T.; methodology, J.T.; formal analysis, J.T.; investigation, J.T.; writing—original draft preparation, J.T.; writing—review and editing, S.B. and M.H. All authors have read and agreed to the published version of the manuscript.

Funding: This research was funded by Austrian Research Promotion Agency (FFG), grant number FO999887928. Open Access Funding by TU Wien.

Informed Consent Statement: Not applicable.

Data Availability Statement: Not applicable.

Acknowledgments: The production of the CLP suspension was carried out in cooperation with Lignovations GmbH, Austria. The contact angle measurement was carried out in cooperation with Oihana Gordobil, InnoRenew CoE, Slovenia. The fluorescence microscopy was carried out using the facilities of the Research Group for Physical Chemistry of Aerosol Particles, TU Wien, Austria. The rheological investigations were carried out using facilities of the Research Group for Polymer Chemistry and Technology, TU Wien, Austria. Scanning electron microscopy image acquisition of the lignin particles was carried out using facilities at the University Service Centre for Transmission Electron Microscopy (USTEM), TU Wien, Austria. The authors acknowledge the TU Wien University Library for financial support through its Open Access Funding Program.

Conflicts of Interest: The authors declare no conflict of interest.

References

1. Lewandowski, I. *Bioeconomy. Shaping the Transition to a Sustainable, Biobased Economy*; Springer International Publishing: Cham, Switzerland, 2018.
2. Kamm, B.; Kamm, M. Principles of biorefineries. *Appl. Microbiol. Biotechnol.* **2004**, *64*, 137–145. [[CrossRef](#)] [[PubMed](#)]
3. Ragauskas, A.J.; Beckham, G.T.; Biddy, M.J.; Chandra, R.; Chen, F.; Davis, M.F.; Davison, B.H.; Dixon, R.A.; Gilna, P.; Keller, M.; et al. Lignin valorization: Improving lignin processing in the biorefinery. *Science* **2014**, *344*, 1246843. [[CrossRef](#)] [[PubMed](#)]

4. Puglia, D.; Santulli, C.; Sarasini, F. *Micro and Nano Lignin in Aqueous Dispersions and Polymers*; Elsevier: Amsterdam, The Netherlands, 2020; Volume 12.
5. Belgacem, M.N.; Gandini, A. *Monomers, Polymers and Composites from Renewable Resources*, 1st ed.; Elsevier: Amsterdam, The Netherlands; Boston, MA, USA, 2008.
6. John, M.J.; Lefatle, M.C.; Sithole, B. Lignin fractionation and conversion to bio-based functional products. *Sustain. Chem. Pharm.* **2022**, *25*, 100594. [[CrossRef](#)]
7. Moreno, A.; Sipponen, M.H. Lignin-based smart materials: A roadmap to processing and synthesis for current and future applications. *Mater. Horiz.* **2020**, *7*, 2237–2257. [[CrossRef](#)]
8. Beisl, S.; Miltner, A.; Friedl, A. Lignin from Micro- to Nanosize: Production Methods. *Int. J. Mol. Sci.* **2017**, *18*, 1244. [[CrossRef](#)]
9. Gordobil, O.; Olaizola, P.; Banales, J.M.; Labidi, J. Lignins from Agroindustrial by-Products as Natural Ingredients for Cosmetics: Chemical Structure and In Vitro Sunscreen and Cytotoxic Activities. *Molecules* **2020**, *25*, 1131. [[CrossRef](#)]
10. Chauhan, P.S.; Agrawal, R.; Satlewal, A.; Kumar, R.; Gupta, R.P.; Ramakumar, S.S.V. Next generation applications of lignin derived commodity products, their life cycle, techno-economics and societal analysis. *Int. J. Biol. Macromol.* **2022**, *197*, 179–200. [[CrossRef](#)]
11. Beisl, S.; Adamczyk, J.; Friedl, A. Direct Precipitation of Lignin Nanoparticles from Wheat Straw Organosolv Liquors Using a Static Mixer. *Molecules* **2020**, *25*, 1388. [[CrossRef](#)]
12. Österberg, M.; Sipponen, M.H.; Mattos, B.D.; Rojas, O.J. Spherical lignin particles: A review on their sustainability and applications. *Green Chem.* **2020**, *22*, 2712–2733. [[CrossRef](#)]
13. Zhao, W.; Simmons, B.; Singh, S.; Ragauskas, A.; Cheng, G. From lignin association to nano-/micro-particle preparation: Extracting higher value of lignin. *Green Chem.* **2016**, *18*, 5693–5700. [[CrossRef](#)]
14. Freitas, F.M.C.; Cerqueira, M.A.; Gonçalves, C.; Azinheiro, S.; Garrido-Maestu, A.; Vicente, A.A.; Pastrana, L.M.; Teixeira, J.A.; Michelin, M. Green synthesis of lignin nano- and micro-particles: Physicochemical characterization, bioactive properties and cytotoxicity assessment. *Int. J. Biol. Macromol.* **2020**, *163*, 1798–1809. [[CrossRef](#)] [[PubMed](#)]
15. Iravani, S.; Varma, R.S. Greener synthesis of lignin nanoparticles and their applications. *Green Chem.* **2020**, *22*, 612–636. [[CrossRef](#)]
16. Adamczyk, J.; Beisl, S.; Amini, S.; Jung, T.; Zikeli, F.; Labidi, J.; Friedl, A. Production and Properties of Lignin Nanoparticles from Ethanol Organosolv Liquors-Influence of Origin and Pretreatment Conditions. *Polymers* **2021**, *13*, 384. [[CrossRef](#)] [[PubMed](#)]
17. Beisl, S.; Friedl, A.; Miltner, A. Lignin from Micro- to Nanosize: Applications. *Int. J. Mol. Sci.* **2017**, *18*, 2367. [[CrossRef](#)]
18. Chevalier, Y.; Bolzinger, M.-A. Emulsions stabilized with solid nanoparticles: Pickering emulsions. *Colloids Surf. A Physicochem. Eng. Asp.* **2013**, *439*, 23–34. [[CrossRef](#)]
19. Yang, Y.; Fang, Z.; Chen, X.; Zhang, W.; Xie, Y.; Chen, Y.; Liu, Z.; Yuan, W. An Overview of Pickering Emulsions: Solid-Particle Materials, Classification, Morphology, and Applications. *Front. Pharmacol.* **2017**, *8*, 287. [[CrossRef](#)]
20. Yu, X.; Chen, S.; Wang, W.; Deng, T.; Wang, H. Empowering alkali lignin with high performance in pickering emulsion by selective phenolation for the protection and controlled-release of agrochemical. *J. Clean. Prod.* **2022**, *339*, 130769. [[CrossRef](#)]
21. Riseh, R.S.; Skorik, Y.A.; Thakur, V.K.; Pour, M.M.; Tamanadar, E.; Noghabi, S.S. Encapsulation of Plant Biocontrol Bacteria with Alginate as a Main Polymer Material. *Int. J. Mol. Sci.* **2021**, *22*, 11165. [[CrossRef](#)]
22. Garg, J.; Chiu, M.N.; Krishnan, S.; Tripathi, L.K.; Pandit, S.; Far, B.F.; Jha, N.K.; Kesari, K.K.; Tripathi, V.; Pandey, S.; et al. Applications of lignin nanoparticles for cancer drug delivery: An update. *Mater. Lett.* **2022**, *311*, 131573. [[CrossRef](#)]
23. Sadeghifar, H.; Ragauskas, A. Lignin as a UV Light Blocker—A Review. *Polymers* **2020**, *12*, 1134. [[CrossRef](#)]
24. Gutiérrez-Hernández, J.M.; Escalante, A.; Murillo-Vázquez, R.N.; Delgado, E.; González, F.J.; Toríz, G. Use of Agave tequilana-lignin and zinc oxide nanoparticles for skin photoprotection. *J. Photochem. Photobiol. B Biol.* **2016**, *163*, 156–161. [[CrossRef](#)] [[PubMed](#)]
25. Miltner, M.; Beisl, S.; Miltner, A.; Adamczyk, J.; Gaspar, R.; Capelo, S.; Harasek, M.; Friedl, A. Application of Membrane Separation of Cleaning and Concentration of Nanolignin Suspensions in a Biorefinery Environment. *Chem. Eng. Trans.* **2019**, *76*, 133–138.
26. Zhang, Z.; Terrasson, V.; Guénin, E. Lignin Nanoparticles and Their Nanocomposites. *Nanomaterials* **2021**, *11*, 1336. [[CrossRef](#)] [[PubMed](#)]
27. Binks, B.P. Particles as surfactants—Similarities and differences. *Curr. Opin. Colloid Interface Sci.* **2002**, *7*, 21–41. [[CrossRef](#)]
28. Bertolo, M.R.; Brenelli de Paiva, L.B.; Nascimento, V.M.; Gandin, C.A.; Neto, M.O.; Driemeier, C.E.; Rabelo, S.C. Lignins from sugarcane bagasse: Renewable source of nanoparticles as Pickering emulsions stabilizers for bioactive compounds encapsulation. *Ind. Crops Prod.* **2019**, *140*, 111591. [[CrossRef](#)]
29. Ago, M.; Huan, S.; Borghesi, M.; Raula, J.; Kauppinen, E.I.; Rojas, O.J. High-Throughput Synthesis of Lignin Particles (~30 nm to ~2 µm) via Aerosol Flow Reactor: Size Fractionation and Utilization in Pickering Emulsions. *ACS Appl. Mater. Interfaces* **2016**, *8*, 23302–23310. [[CrossRef](#)]
30. Radotić, K.; Kalauzi, A.; Djikanović, D.; Jeremić, M.; Leblanc, R.M.; Cerović, Z.G. Component analysis of the fluorescence spectra of a lignin model compound. *J. Photochem. Photobiol. B Biol.* **2006**, *83*, 1–10. [[CrossRef](#)]
31. Hochstein, B.; Brummer, R. *Rheologische Grundlagen und Relevanz in der Kosmetischen Industrie*; Karlsruhe Institute of Technology: Karlsruhe, Germany, 2012.
32. Hohl, L.; Röhl, S.; Stehl, D.; von Klitzing, R.; Kraume, M. Influence of Nanoparticles and Drop Size Distributions on the Rheology of w/o Pickering Emulsions. *Chem. Ing. Tech.* **2016**, *88*, 1815–1826. [[CrossRef](#)]

33. Leuprecht, P. Determination of the Mechanical and Thermal Stability of Skin Cream with Oscillation and Freeze-Thaw Cycle Tests.
34. Torres, L.G.; Iturbe, R.; Snowden, M.J.; Chowdhry, B.Z.; Leharne, S.A. Preparation of o/w emulsions stabilized by solid particles and their characterization by oscillatory rheology. *Colloids Surf. A Physicochem. Eng. Asp.* **2007**, *302*, 439–448. [[CrossRef](#)]
35. Tadros, T. Application of rheology for assessment and prediction of the long-term physical stability of emulsions. *Adv. Colloid Interface Sci.* **2004**, *108–109*, 227–258. [[CrossRef](#)]
36. Derkach, S.R. Rheology of emulsions. *Adv. Colloid Interface Sci.* **2009**, *151*, 1–23. [[CrossRef](#)] [[PubMed](#)]

Disclaimer/Publisher's Note: The statements, opinions and data contained in all publications are solely those of the individual author(s) and contributor(s) and not of MDPI and/or the editor(s). MDPI and/or the editor(s) disclaim responsibility for any injury to people or property resulting from any ideas, methods, instructions or products referred to in the content.